# Calcium Phosphate Incorporated Poly(ethylene oxide)-Based Nanocomposite Electrolytes for Lithium Batteries. I. Ionic Conductivity and Positron Annihilation Lifetime Spectroscopy Studies

**A. Manuel Stephan,[1] T. Prem Kumar,[1] Sabu Thomas,[2] P. Selvin Thomas,[2] Roberta Bongiovanni,[3] Jijeesh R. Nair,[3] N. Angulakshmi[1]**

[1]*Electrochemical Power Systems Division, Central Electrochemical Research Institute, Karaikudi 630 006, India*
[2]*School of Chemical Sciences, Mahatma Gandhi University, Kottayam 68 65 60, India*
[3]*Department of Materials Science and Chemical Engineering, Politecnico di Torino c. Duca degil Abruzzi 24 10129, Torino, Italy*

Received 22 November 2010; accepted 17 June 2011
DOI 10.1002/app.35219
Published online 18 November 2011 in Wiley Online Library (wileyonlinelibrary.com).

**ABSTRACT:** Nanocomposite polymer electrolytes (NCPEs) composed of poly(ethylene oxide), calcium phosphate [$Ca_3(PO_4)_2$], and lithium perchlorate ($LiClO_4$)/lithium bis(trifluoromethane sulfonyl)imide [$LiN(CF_3SO_2)_2$ or LiTFSI] in various proportions were prepared by a hot-press method. The membranes were characterized by scanning electron microscopy, differential scanning calorimetry, thermogravimetry–differential thermal analysis, ionic conductivity testing, and transference number studies. The free volume of the membranes was probed by positron annihilation lifetime spectroscopy at 30°C, and the results supported the ionic conductivity data. The NCPEs with $LiClO_4$ exhibited higher ionic conductivities than the NCPE with LiTFSI as a salt. © 2011 Wiley Periodicals, Inc. J Appl Polym Sci 124: 3245–3254, 2012

**Key words:** composites; FT-IR; thermogravimetric analysis (TGA)

## INTRODUCTION

The development of polymer electrolytes has long been the subject of research interest because of their potential applications, not only in the area of rechargeable lithium batteries but also in other electrochemical devices.[1–3] Commercially available lithium-ion cells possess a lithium-intercalating polycrystalline oxide as the cathode and a carbon anode with a nonaqueous liquid electrolyte. The development of polymer electrolytes for lithium batteries has led to an unprecedented interest in the last 2 decades because of their potential advantages, such as nonleakage of electrolyte, high energy density, flexible geometry, and better safety.[4,5]

The ionic conductivity of dry polymer electrolytes has been found to be on the order of $10^{-4}$ S/cm at temperatures above 90°C, which excludes them from practical applications.[5] In the last 3 decades, numerous attempts have been made to improve the ionic conductivity of polymeric membranes at ambient and subambient temperatures through the addition of low-molecular-weight plasticizers, such as ethylene carbonate and propylene carbonate. However, the incorporation of plasticizers adversely affects the mechanical robustness of membranes and the interfacial properties with lithium metal anodes and eventually deteriorates the system.[6,7]

Recent studies have revealed that only ceramic/inert filler (e.g., $ZrO_2$, $SiO_2$, $Al_2O_3$) incorporated composite polymer electrolytes can offer safe and reliable batteries.[8–10] The concept of incorporating inert fillers into polymer–LiX salt complexes is not new. This procedure has already been adopted successfully to enhance the mechanical stability (brought about by a network of filler particles in the polymer matrix), improve the compatibility of solid polymer electrolytes with lithium metal anodes, and achieve a high ionic conductivity.[10]

A variety of polymer hosts have been studied. Among the polymer hosts explored so far, poly(ethylene oxide) (PEO) has been the most extensively studied system because of its ability to form complexes with a wide variety of lithium salts for battery applications. PEO chains adopt a helical conformation with all the C—O bonds in trans configuration and the C—C bonds in either the gauche or gauche minus configuration.[11] In this

*Correspondence to:* A. M. Stephan (arulmanuel@gmail.com).

Contract grant sponsor: Department of Science and Technology, New Delhi, through an SERC scheme.

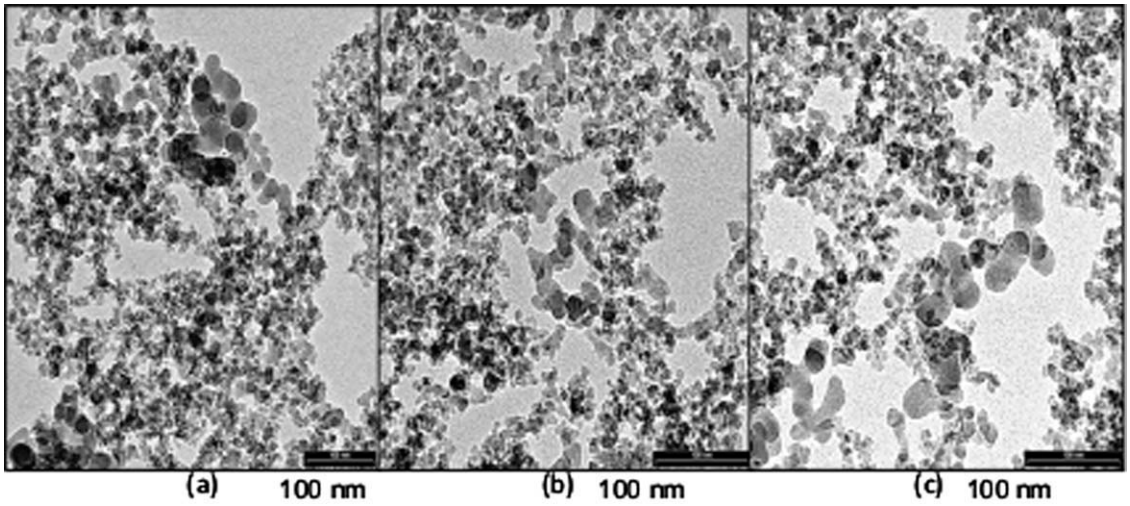


**Figure 1** TEM images of the $Ca_3(PO_4)_2$ nanoparticles: PEO/$CaCl_2$ ratio: (a) 2 : 1, (b) 4 : 1, and (c) 5 : 1.

geometry, cations can be located in each turn of the helix and are coordinated by three ether oxygens. However, the basic structure of the host is retained for all sizes of anions. In this study, nanosized calcium phosphate [nano-$Ca_3(PO_4)_2$] was used as a filler. To the best of our knowledge, nano-$Ca_3(PO_4)_2$ has never been investigated as a filler in nanocomposite polymer electrolytes (NCPEs). Studies have indicated that membranes prepared by the conventional solvent casting method lead to poor interfacial properties at the lithium/polymer electrolyte interface.[12] Impurities, mostly traces of solvent, are trapped in the high-surface-area, nanosized inert fillers in solvent-cast electrolytes and are present even after prolonged drying.[13] Hence, in this study, the hot-press technique was used for the preparation of the NCPEs.

## EXPERIMENTAL

### Preparation of nano-$Ca_3(PO_4)_2$

The nano-$Ca_3(PO_4)_2$ filler particles were synthesized with an *in situ* deposition technique in the presence of PEO, as reported by one of us.[14] First, a complex of calcium chloride with PEO (Aldrich, USA) was prepared in desired proportions in methanol. An appropriate stoichiometric amount of trisodium phosphate [$Na_3(PO_4)$] in distilled water was added to this complex slowly without stirring. The whole mixture was allowed to digest at room temperature for 24 h, when both the chloride and phosphate ions diffused through the PEO and formed a white gel-like precipitate, which was filtered, washed, and dried. The samples were prepared for different molar concentrations of the PEO–$CaCl_2$ complex of 2 : 1, 4 : 1, and 5 : 1, and the yields of $Ca_3(PO_4)_2$ were recorded as 83, 75, and 67%, respectively. The prepared compound was washed with double-distilled water several times until it reached a pH value of 7 to remove Na from the final product. Figure 1 shows the transmission electron microscopy (TEM) images of $Ca_3(PO_4)_2$ prepared with different compositions of PEO. However, in this study, the sample prepared with a ratio of PEO to $CaCl_2$ of 4 : 1 was used. Figure 2 depicts the particle size distribution of the $Ca_3(PO_4)_2$ nanoparticles. Around 400 particles were taken for the analysis, and a very narrow distribution of particles was seen. The average particle size of the synthesized $Ca_3(PO_4)_2$ particles was found to be less than 20 nm.

### Preparation of the NCPEs

PEO (Aldrich) and lithium perchlorate ($LiClO_4$; Merck, Germany) were dried *in vacuo* for 2 days at 50 and 100°C, respectively. The prepared $Ca_3(PO_4)_2$, as described earlier, was also dried *in vacuo* at 50°C

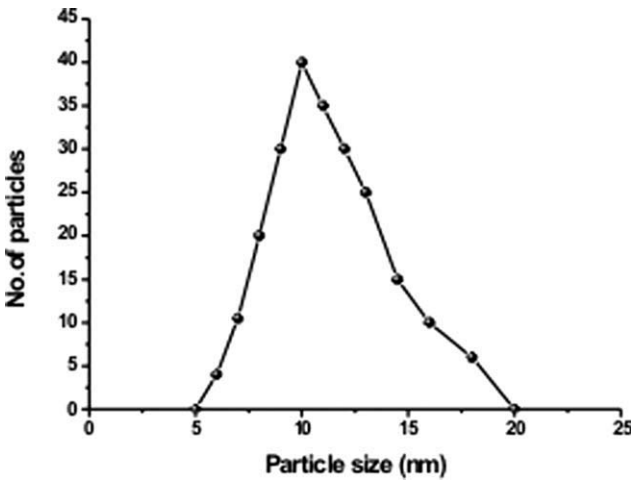


**Figure 2** Particle size distribution of the $Ca_3(PO_4)_2$ nanoparticles.

**TABLE I**
**Compositions of the Polymer, $Ca_3(PO_4)_2$, and Lithium Salt**

| Sample | Polymer (wt %) | $Ca_3(PO_4)_2$ (wt %) | $LiClO_4/LiN(CF_3SO_2)_2$ (wt %) |
|---|---|---|---|
| S1 | 95 | 0 | 5 |
| S2 | 90 | 5 | 5 |
| S3 | 85 | 10 | 5 |
| S4 | 75 | 17 | 8 |
| S5 | 70 | 20 | 10 |
| S6 | 94 | 5 | 1 |
| S7 | 93 | 5 | 2 |
| S8 | 92 | 5 | 3 |
| S9 | 91 | 5 | 4 |

for 5 days before use. Nanocomposite electrolytes were prepared by the dispersion of appropriate amounts of $Ca_3(PO_4)_2$ in PEO–$LiClO_4$/lithium bis(-trifluoromethane sulfone)imide [$LiN(CF_3SO_2)_2$ or LiTFSI; Table I], and the powder was hot-pressed into films, as described elsewhere.[12,13] The nanocomposite electrolyte films had an average thickness of 30–50 μm and were measured with a digital micrometer (Mitutoyo, Japan). This procedure yielded homogeneous and mechanically strong membranes, which were dried *in vacuo* at 50°C for 24 h for further characterization.

### Electrochemical characterization

The ionic conductivity of the membranes sandwiched between two stainless steel blocking electrodes (1 cm in diameter) was measured with an electrochemical impedance analyzer (IM6-Bio Analytical Systems, Germany) in the 50 mHz–100 kHz frequency range at various temperatures (0, 15, 30, 40, 50, 60, 70, and 80°C) with an accuracy of ± 0.1°C. Symmetric nonblocking cells of the type Li/composite polymer electrolytes (CPE)/Li were assembled for compatibility studies and were investigated by the study of the time dependence of the impedance of the systems under an open circuit at 60°C.

The lithium transference number was calculated by the method proposed by Bruce et al.[15] The following formula was adopted to measure the lithium transference number ($t_{Li}^+$):[16]

$$t_{Li}{}^+ = \frac{I_{ss}(V - I_0R_0)}{I_0(V - I_{ss}R_{ss})} \quad (1)$$

where $V$ is applied potential.

The Li/NCPE/Li cell was polarized by a direct-current pulse of 10 mV. The time evolution of the resulting current flow was then followed. The initial and steady-state values of current ($I_0$ and $I_{ss}$, respectively) flowing through the cell during the polarization were measured. $R_0$ and $R_{ss}$ represent the resistance values before and after the perturbation of the system, respectively. Impedance spectra were made before and after the pulse application to correct the changes.

Morphological examination of the films was made by a field-emission scanning electron microscope (S-4700, Hitachi, Japan) under vacuum conditions ($10^{-1}$ Pa) after gold was sputtered on one side of the films. Differential scanning calorimetry (DSC; Mettler Toledo, Switzerland) measurements were performed at a rate of 10°C/min between 20 and 250°C with thermogravimetry (TG)–differential thermal analysis (DTA) in the temperature range 20–300°C. The lithium/polymer electrolyte interface was analyzed with Fourier transform infrared (FTIR) spectroscopy (Thermo Nicolet Corp., Nexus model 670) by single-internal-reflection mode.[17] The infrared spectra were obtained at ambient temperature with an 8-$cm^{-1}$ resolution. Positron annihilation lifetime spectroscopy (PALS) measurements were made with a $^{22}Na$ source with a resolution of 250 ps. The data were collected at 30°C on a 70-μm thick nanocomposite polymer membrane, and the spectrum was analyzed by PATFIR-88 program (USA).

## RESULTS AND DISCUSSION

### Thermal analysis

Figure 3(a–d) shows the DSC thermograms of samples PEO + LiTFSI, PEO + $Ca_3(PO_4)_2$ + LiTFSI, PEO + $LiClO_4$, and PEO + $Ca_3(PO_4)_2$ + $LiClO_4$, respectively. The melting endothermic peak of PEO + LiTFSI (66°C) [Fig. 3(b)] decreased and broadened upon the incorporation of $Ca_3(PO_4)_2$ into the polymer matrix. The broadening of the endothermic peak accompanied a decrease in the heat of fusion,

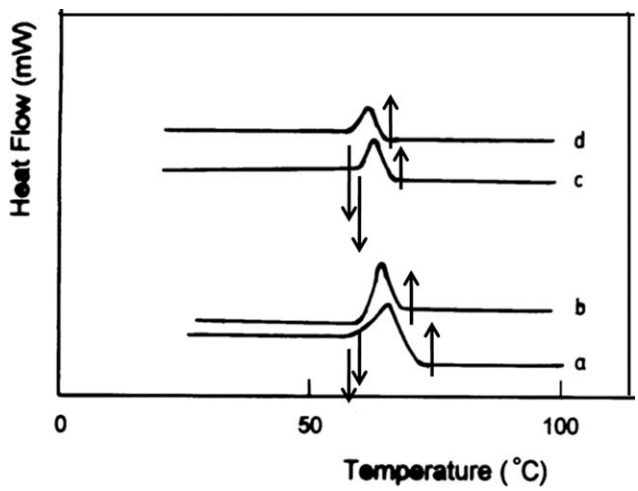


**Figure 3** DSC thermograms of (a) PEO + LiTFSI, (b) PEO + LiTFSI + $Ca_3(PO_4)_2$, (c) PEO + $LiClO_4$, and (d) PEO + $LiClO_4$ + $Ca_3(PO_4)_2$.

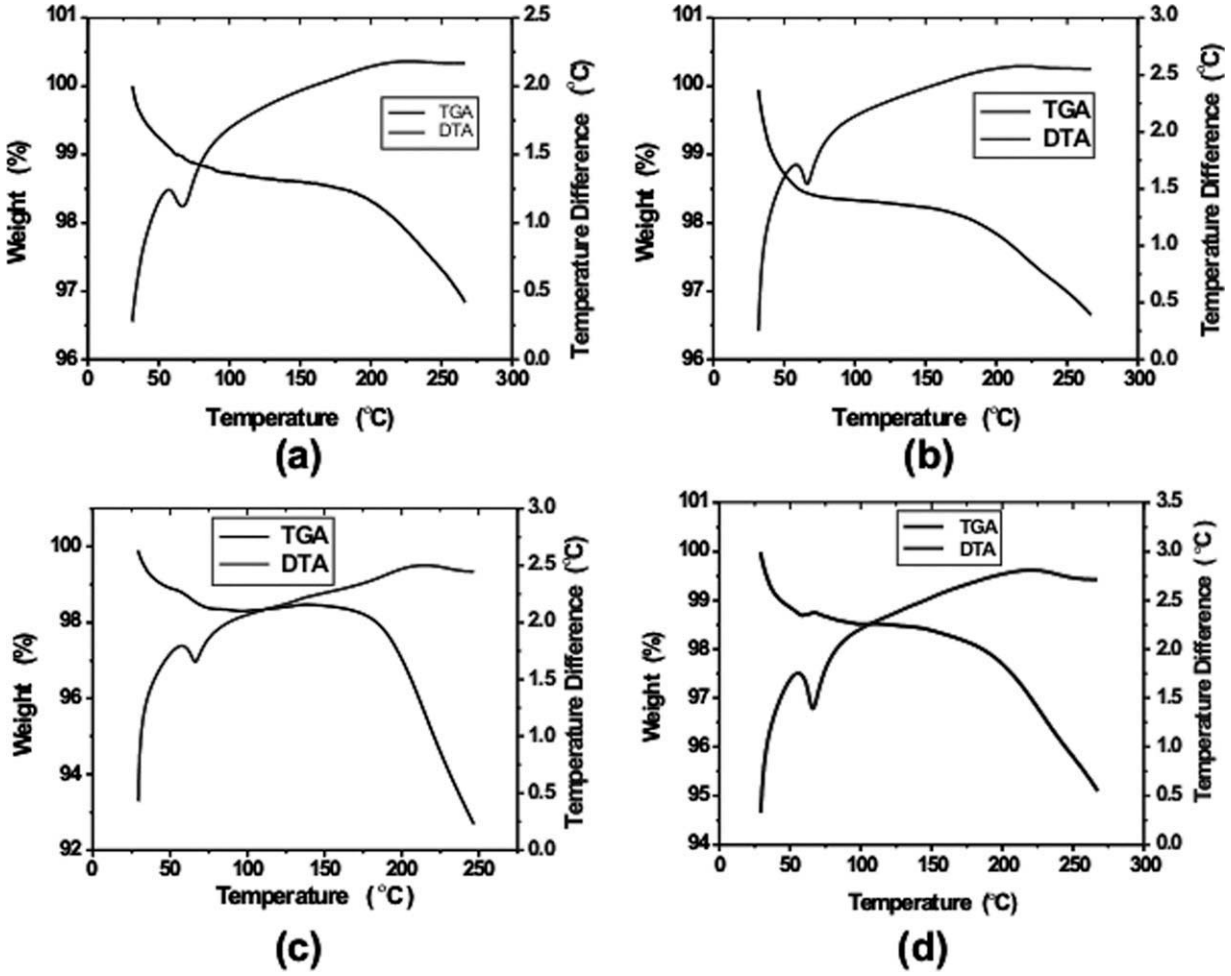


**Figure 4** TG–DTA traces of (a) PEO + LiTFSI, (b) PEO + $Ca_3(PO_4)_2$ + LiTFSI, (c) PEO + $LiClO_4$, and (d) PEO + $Ca_3(PO_4)_2$ + $LiClO_4$.

which increased with the concentration of $Ca_3(PO_4)_2$.[18] A similar trend was observed for $LiClO_4$-laden samples also. The TG–DTA traces of PEO + LiTFSI, PEO + LiTFSI + $Ca_3(PO_4)_2$, PEO + $LiClO_4$, and PEO + $LiClO_4$ + $Ca_3(PO_4)_2$ are depicted in Figure 4(a–d). An endothermic peak was seen in all four samples around 37°C and was attributed to the presence of moisture at the time of loading the samples.[19] An observed weight loss of about 2% [Fig. 4(a)] was attributed to the removal of superficial water from the sample. As pointed out in the DSC results, the broadening of the endothermic peak was attributed to both the decrease in the heat diffusion and the removal of superficial water. Further, no weight loss was observed until an irreversible decomposition took place at around 180°C. However, in the $Ca_3(PO_4)_2$-incorporated samples [Fig. 4(b)], the onset of the irreversible decomposition process shifted marginally to a higher temperature (195°C); this suggested strong and more intensive bonding between the filler and the polymer host.[18,19] This was attributed to the intercalation/exfoliation of the polymer matrix with inert particles, which resulted in a strong barrier effect, which prevented thermal degradation to a certain extent. This observation was an indication of the fact that PEO + LiTFSI + $Ca_3(PO_4)_2$ was stable up to a temperature of 294°C in a nitrogen atmosphere.[20]

A similar trend was observed with $LiClO_4$-added NCPE. Irreversible decompositions started for PEO + $LiClO_4$ and PEO + $Ca_3(PO_4)_2$ + $LiClO_4$ [Fig. 4(c,d)] around 185 and 190°C, respectively. The thermal stability of the composite polymer electrolyte with LiTFSI was found to be higher than that of $LiClO_4$, and this was attributed to the higher melting point of LiTFSI (236°C).[21]

### Scanning electron microscopy (SEM) analysis

Figure 5(a–d) shows typical SEM images of the PEO + LiTFSI (sample S1), PEO + LiTFSI + $Ca_3(PO_4)_2$ (sample S5), PEO + $LiClO_4$ (sample S1), and PEO + $LiClO_4$ + $Ca_3(PO_4)_2$ (sample S5) membranes, respectively. Figure 5(a) reveals a smooth morphology

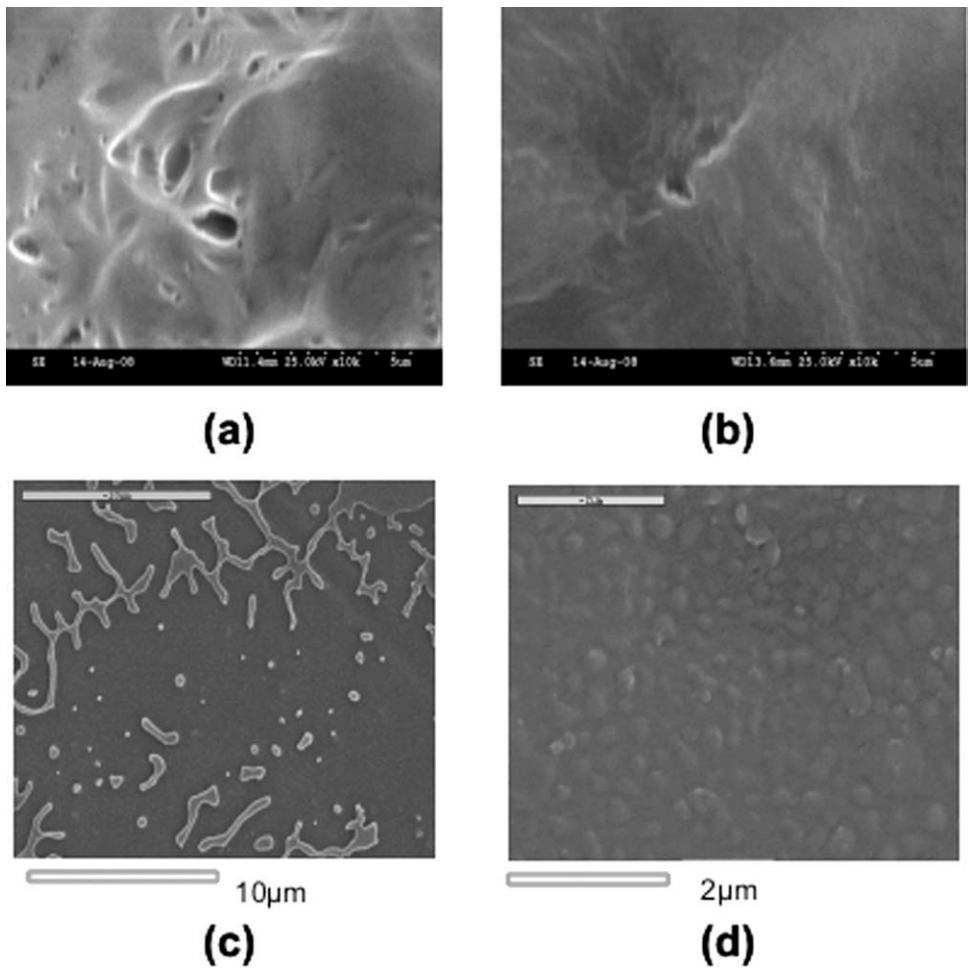


**Figure 5** SEM images of (a) PEO + LiTFSI, (b) PEO + $Ca_3(PO_4)_2$ + LiTFSI, (c) PEO + $LiClO_4$, and (d) PEO + $Ca_3(PO_4)_2$ + $LiClO_4$.

with some cavities. On the other hand, a rough surface was seen with an inhomogeneous morphology composed of islands of aggregated particles upon the incorporation of $Ca_3(PO_4)_2$ into the polymer matrix [Fig. 5(b,d)]. This was attributed to a reduction in the crystallinity of the PEO due to crosslinking with cations of both lithium ions and $Ca_3(PO_4)_2$.[22] We observed an island of like structure, as shown in Figure 4(c) (PEO + $LiClO_4$), as a result of the heterogeneous nature of the system. A similar morphology was obtained by Chu and coworkers,[22,23] who reported morphological studies of PEO–$SiO_2$ complexes.

### Ionic conductivity

The temperature dependence of NCPEs as a function of the LiTFSI concentration and $Ca_3(PO_4)_2$ is shown in Figure 6(a,b), respectively. It is quite obvious from both figures that the ionic conductivity of the composite polymer electrolyte increased with increasing temperature and also increasing salt content.[24–26] The ionic conductivity also increased with increasing filler content up to 10 wt % and then decreased with further increasing filler content. The ionic conductivity of the polymer membrane increased to one order of magnitude upon the addition of filler in the polymer matrix. These results were in accordance with those reported earlier, in which $Al_2O_3$ was used as a filler in PEO-based electrolytes.[27] A similar trend was observed for the polymer electrolytes with $LiClO_4$ as a salt [Fig. 6(c,d)].

As commonly observed in composite materials, the conductivity was not a linear function of filler concentration. At low concentration, the dilution effect, which tends to depress the ionic conductivity, was effectively contrasted by the specific interactions of the ceramic surfaces, which promoted faster ion transport. Hence, an apparent enhancement in conductivity was seen in both cases.[24] On the other hand, at higher filler concentrations, the dilution effect predominated, and the conductivity decreased. Thus, the maximum conductivity was achieved only in the concentration region of 8–10 wt %. These

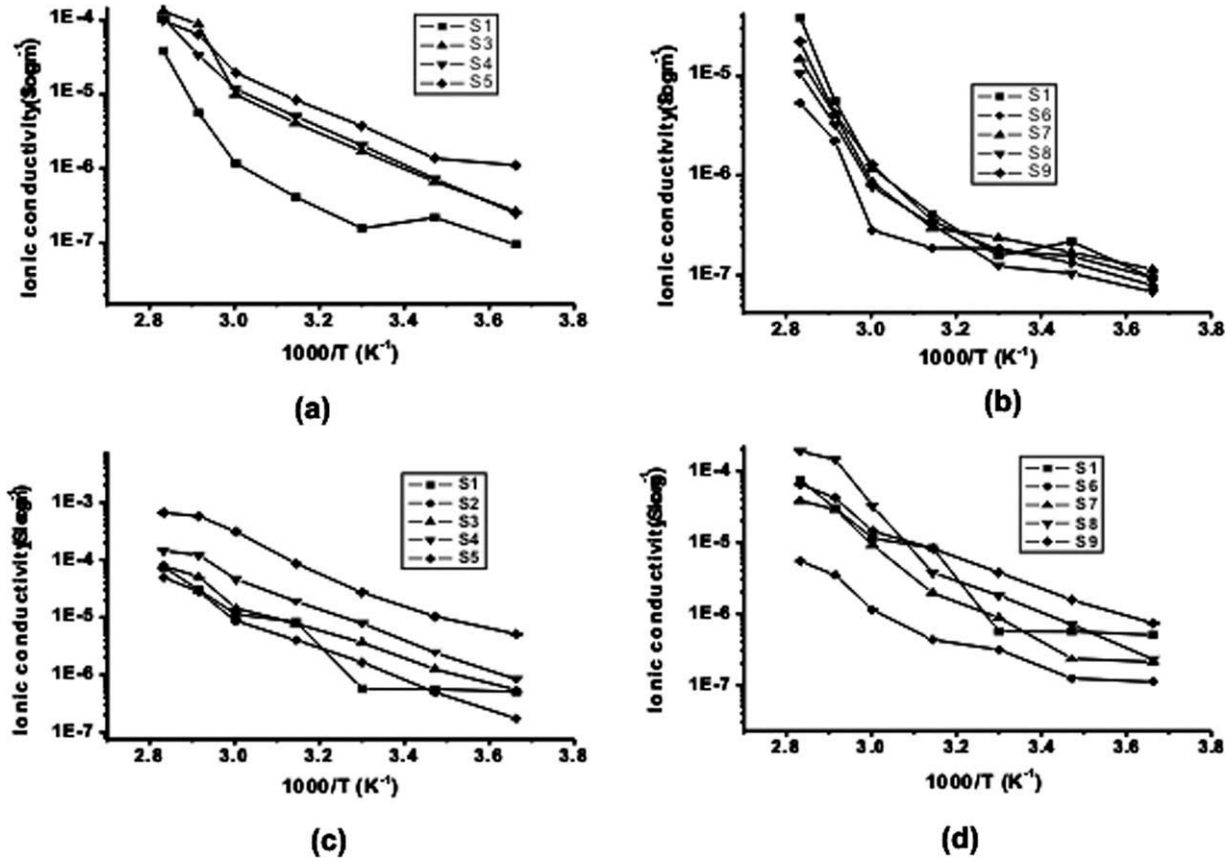


**Figure 6** Ionic conductivity as a function of the temperatures for (a) PEO + LiTFSI, (b) PEO + $Ca_3(PO_4)_2$ + LiTFSI, (c) PEO + $LiClO_4$, and (d) PEO + $Ca_3(PO_4)_2$ + $LiClO_4$.

results were in accordance with those reported for PEO-based polymer electrolytes with lithium imide anions.[25,26,28]

According to Wieczorek and coworkers,[29,30] the Lewis base reactions between the filler surface and the PEO segments may induce structural modifications in the polymer matrix. The Lewis acid character of the added ceramics would compete with the Lewis acid character of the of the lithium cations for the formation of complexes with the PEO chains. In general, the filler that has a basic center will react with the Lewis acid centers of the polymer chain, and these interactions will lead to the reduction in the crystallinity of the polymer host. In this study, $PO_4^{3-}$ could act as a crosslinking center for the PEO segments, which lowered the polymer chain reorganization tendency and promoted an overall stiffness in the structure. However, the resulting structure provided $Li^+$ -conducting pathways at the filler surface and enhanced ionic transport.

### Effect of anions on the ionic conductivity

To determine the effect of the anion, a comparison was made on the NCPEs with sample S1 and S5 with $LiClO_4$ and LiTFSI, respectively, as the salts, as shown in Figure 7. The NCPE with $LiClO_4$ as the salt exhibited a higher ionic conductivity at all temperatures than that of the membranes with LiTFSI. Because both anions were counter ions of strong acids and were sterically encumbered, the differences in the ionic conductivity were presumably due to the difference in the lattice energies.[31] However, the conductivity order based on anion type is not fully understood for both liquid and polymer electrolytes for lithium batteries. The conductivity can be affected by the ionic mobility, ion–ion interactions, anion size, lattice energies, salt dissociation, and also anion polarization, all of which depend on salt concentration.[32]

### Lithium transference number

Although a high ionic conductivity, enhanced thermal stability, and good compatibility with lithium electrodes are desirable properties, they are not sufficient to make a membrane useful for practical applications. The transference numbers in polymer electrolytes play an important role in clarifying the mechanisms of ion transport and partly predict the performance of practical battery systems. A variety of approaches have been used, which include Hittorf

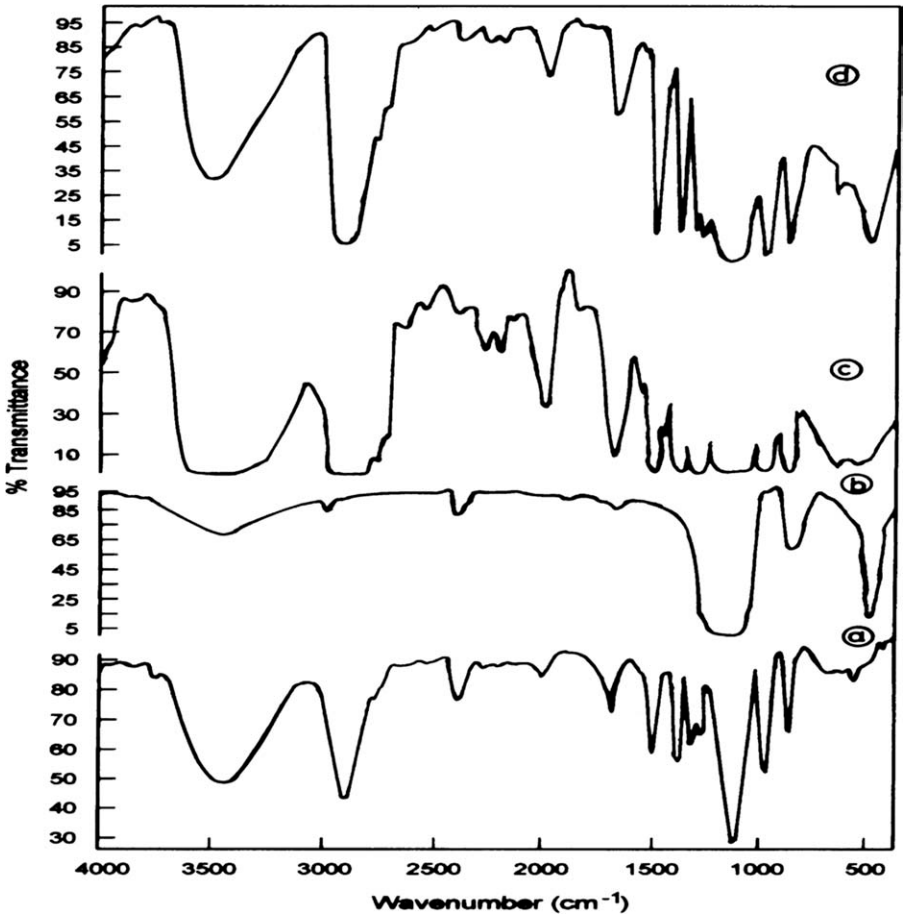


**Figure 7** FTIR spectra of (a) PEO, (b) $Ca_3(PO_4)_2$, (c) PEO + LiTFSI, and (d) PEO + $Ca_3(PO_4)_2$ + LiTFSI.

or moving boundary, pulsed-field gradient NMR, and alternating-current impedance ($I_{ss}$) analysis.[33] To understand the effectiveness of $Ca_3(PO_4)_2$ in enhancing the ionic conductivity, transference number studies were carried out on samples S1 and S5 at 60°C, a temperature that was found to be optimal from a conductivity point of view for practical applications. The $Li^+$ transference numbers for samples S1 and S5 were found to be 0.24 and 0.40 with LiTFSI and 0.34 and 0.64 with $LiClO_4$, respectively. The cationic transference numbers were low for the S1 samples because of the strong cation–polymer interactions that existed and the tendency for intermolecular salvation to occur.[34] On the other hand, the $Ca_3(PO_4)_2$-incorporated polymer electrolytes exhibited higher transference numbers. According to Capiglia et al.[28] who reported the transference numbers in the $P(EO)_{20}$–LiBETI–$SiO_2$ system, the increase in the transference number for $Li^+$ ions was due to moisture trapped in the nanoparticles of $SiO_2$. In this study, because the NCPEs were prepared by a hot-press technique with dry constituents, the increase in the transference number may have been due to increased salt dissociation due to the formation of ion–phosphate complexes by Lewis acid–base interactions between the surface groups and the phosphate anions.[26]

## FTIR analysis

FTIR spectroscopy has been identified as a powerful tool for studying the complexation between salts and polymers because of its high sensitivity to molecular and structural changes in polymer electrolyte systems. Figure 8(a–d) shows, respectively, the IR spectra of PEO, $Ca_3(PO_4)_2$, PEO + $LiClO_4$, and PEO + $Ca_3(PO_4)_2$ + $LiClO_4$. The band [Fig. 8(a)] that appeared at 2886 $cm^{-1}$ could be assigned to the —C—H stretching mode of the polymeric chain, and the peak at 1967 $cm^{-1}$ could be assigned to an asymmetric stretching mode. The peaks at 1466, 1103, 956, and 841 $cm^{-1}$ were assigned to —$CH_2$— scissoring, —C—O—C— stretching, —$CH_2$ twisting, and —$CH_2$— wagging modes, respectively.[35] Also, PEO exhibited —C—H stretching (2800–2935 $cm^{-1}$), asymmetric stretching (1950–1970 $cm^{-1}$), asymmetric bending (1450 $cm^{-1}$), $CH_2$ scissoring (1465–1485 $cm^{-1}$), C—O—C stretching (1250–950 $cm^{-1}$), —$CH_2$— twisting (991 $cm^{-1}$), and —$CH_2$— wagging (842 $cm^{-1}$).[35,36]

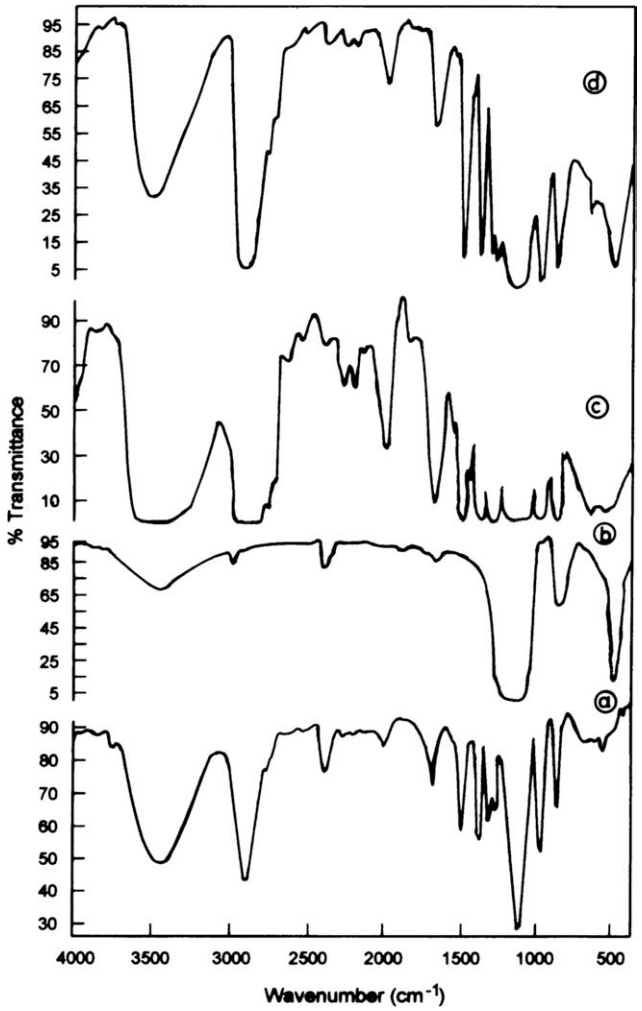


**Figure 8** FTIR spectra of (a) PEO, (b) $Ca_3(PO_4)_2$, (c) PEO + LiTFSI, and (d) PEO + $Ca_3(PO_4)_2$ + LiTFSI.

The C—H bending and rocking modes around 1460 and 850 $cm^{-1}$, respectively, were quite sensitive to the lithium salt complexation upon its incorporation [Fig. 8(c)]. The C—H stretching band centered around 2900 $cm^{-1}$ also exhibited a similar trend. Changes in the peaks [Fig. 8(d)] around 820, 1420–1500, and 2800 $cm^{-1}$ thus indicated complex formation.[37] The FTIR spectra of PEO, $Ca_3(PO_4)_2$, PEO + $LiClO_4$, and PEO + $Ca_3(PO_4)_2$ + $LiClO_4$ are depicted in Figure 9(a–d). Upon incorporation of $LiClO_4$ in the polymer host, the peak at 956 $cm^{-1}$ widened and shifted to 961 $cm^{-1}$. In a similar way, the characteristic frequencies of $LiClO_4$ at 1300 and 920 $cm^{-1}$ shifted, respectively, to 1350 and 940 $cm^{-1}$. The intensity of the peak observed at 2400 $cm^{-1}$ [Fig. 9(b)] was narrowed/reduced further upon incorporation of $Ca_3(PO_4)_2$ [Fig. 9(d)]; this indicated complex formation in the system.[38–40] The shifts in their corresponding characteristic frequencies were attributed to changes in the environment of $—ClO_4^-$. These results were in accordance with those of Ramesh et al.,[36] who reported the interactions of different lithium salts with the PEO matrix.

## PALS studies

The free volume ($V_f$) that arises in polymers because of irregular molecular packing in the amorphous phase may generally be defined as follows:[41]

$$V_f = V_t - V_0 \tag{2}$$

where $V_t$ and $V_0$ represent the total volume and free volume, respectively. Although techniques such as small-angle X-ray scattering,[41] scanning tunneling microscopy, atomic force microscopy,[42,43] SEM, and TEM[44] have been widely employed to determine $V_f$ and the relaxation time, diffraction methods can hardly probe hole sizes below 10 Å.[41,42] PALS has been identified as a powerful tool because of its sensitivity and amenability to *in situ* measurements. Generally, PALS gives three types of lifetime components in polymeric systems. $\tau_1$ relates to parapositronium self-annihilation, whereas $\tau_2$ and $\tau_3$, respectively, relate the free positron and positron/molecular species annihilation and *ortho*-positronium pickoff annihilation. Each lifetime corresponds to an

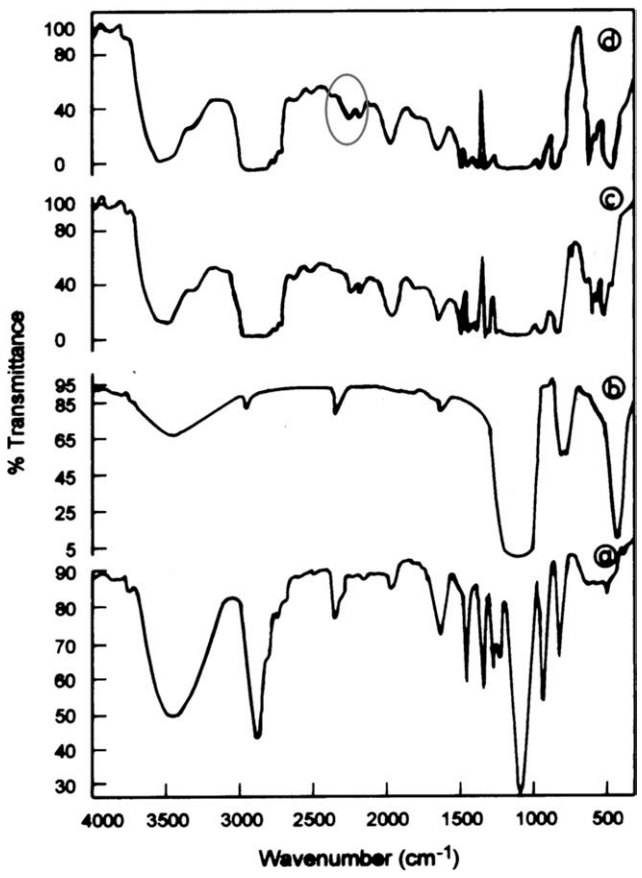


**Figure 9** FTIR spectra of (a) PEO, (b) $Ca_3(PO_4)_2$, (c) PEO + LiTFSI, and (d) PEO + $Ca_3(PO_4)_2$ + LiTFSI.

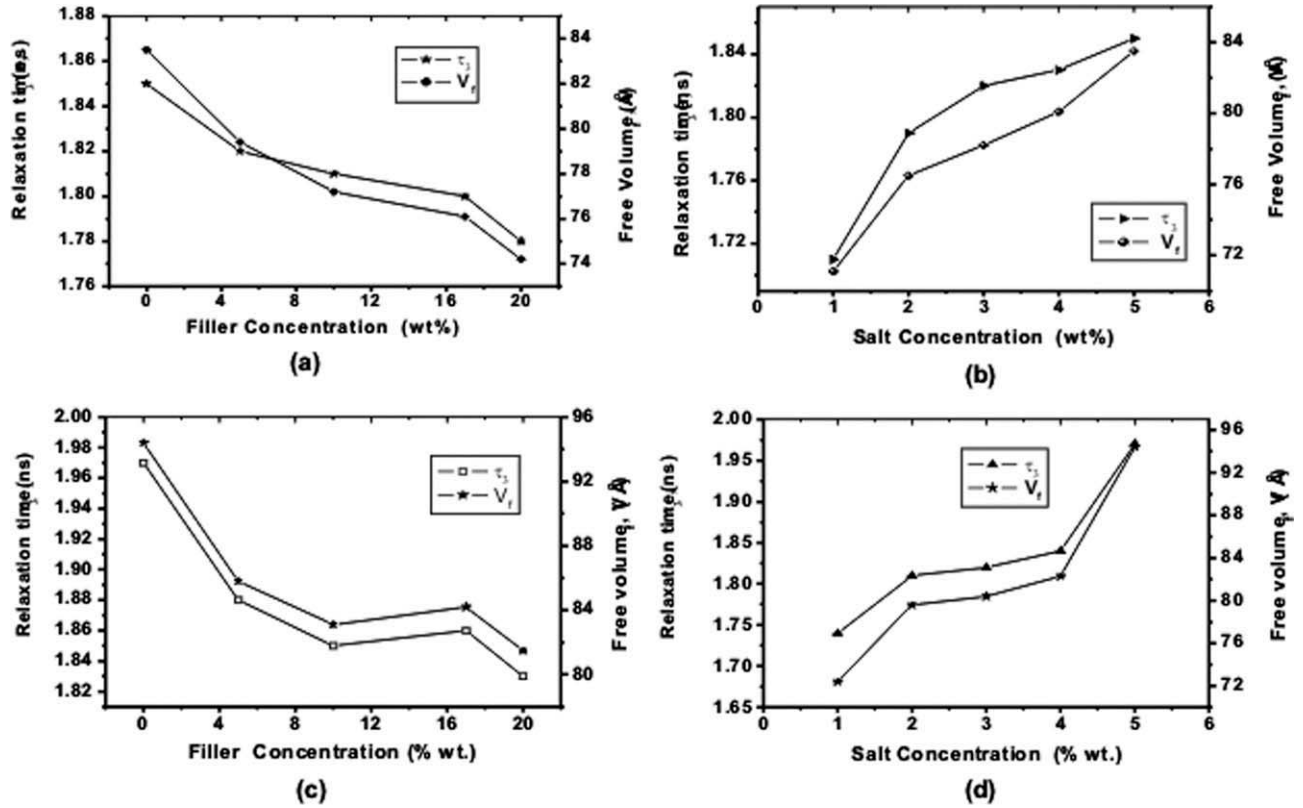


**Figure 10** Variation of $V_f$ and $\tau_3$ (a) as a function of $Ca_3(PO_4)_2$ for fixed LiTFSI, (b) as a function of LiTFSI for fixed $Ca_3(PO_4)_2$, (c) as a function of $Ca_3(PO_4)_2$ for fixed $LiClO_4$, and (d) as a function of $LiClO_4$ for fixed $Ca_3(PO_4)_2$.

intensity ($I_i$), which indicates the relative number of annihilations taking place with a particular lifetime. However, for polymeric materials, the third component ($\tau_3$), with a corresponding $I_3$, is of great interest because of its dependence on $V_f$.[41]

According to the $V_f$ model,[41,42] in the absence of any positron and/or positronium interactions, the inhibition of Ps formation and the quenching of *ortho*-positronium lifetime affects the parameters $\tau_3$ and $I_3$, which may be related, respectively, to the mean radius of the $V_f$ cavities and the relative concentration of holes present in the amorphous regions of the polymer systems. Obviously, $\tau_3$ can be directly correlated to the $V_f$ radius ($R$; Å) by the semiempirical formula:[42]

$$\tau_3 = 1/\lambda_3 = 1/2[1 - R/R_0 + 1/2 \sin(2R/R_0)]^{-1} \quad (3)$$

The spherical cavity volume can be calculated by

$$V_f = 4/3R^3 \quad (4)$$

The $V_f$ sites can be classified in to two categories, namely, (1) static or interstitial and (2) dynamic $V_f$'s. The static $V_f$'s remain as holes, which facilitate the flow of polymer chains. However, dynamic $V_f$ is a time-dependent fraction of the total $V_f$, and the ratio between the static and dynamic $V_f$'s has been found to be greater than 1 and is also temperature dependent. The variation of $V_f$ and $\tau_3$ as a function of salt concentration has been reported by several authors.[41,42] However, the variation of $V_f$ and $\tau_3$ as a function of the composition of nanofiller-added polymer electrolytes has hardly been explored.

Figure 10(a–d) illustrates the variation of $V_f$ and $\tau_3$ as a function of $Ca_3(PO_4)_2$ and LiTFSI and $LiClO_4$. A few plasticization and antiplasticization effects have been reported, in which either a decrease or no change in the amount of $V_f$ below $T_g$ has been observed upon the addition of a plasticizer.[40,43] According to Forsyth et al.,[43] antiplasticization takes place at low concentrations of fillers/plasticizers; this reduces the mobility of amorphous chains. This is attributed to the reduction in the mixture of $V_f$ and to a contribution from the absolute $V_f$ of the plasticizer. It can be seen from Figure 10(a,b) that both $V_f$ and $\tau_3$ decreased significantly up to 10 wt % and then remained approximately more or less the same. A similar trend was observed in the case of Figure 10(c,d) when $LiClO_4$ was used. As the $Li^+$, $ClO_4^-$, and $N(CF_3SO_2)_2^-$ ions were unable to promote inhibition or quenching effects, the observed decreases of $V_f$ and $\tau_3$ were attributed to a decrease in the mean radius of the free-volume cavities of the amorphous phases, which was probably due to the coordination of the $Li^+$ ions in the solvating sites of

the polymer.[39,43–45] The increases of $V_f$ and relaxation time with the increase of lithium salt concentration exactly reflected the ionic conductivity data. Similar observations were reported by Furtado et al.[41] and Forsyth et al.,[43] where the authors probed the lifetime properties of polyurethane-based electrolytes by PALS. However, the role of the anion and the increase and decrease in the $V_f$ have to be clearly understood.

## CONCLUSIONS

PEO-based nanocomposite electrolytes with different compositions of $Ca_3(PO_4)_2$ and lithium salt, $LiClO_4$/$LiN(CF_3SO_2)_2$, were prepared by a hot-press method. Both the ionic conductivity and lithium transference number increased upon the incorporation of $Ca_3(PO_4)_2$ into the polymer matrix. Under open-circuit conditions, the value of the interfacial resistance was found to be lower for $Ca_3(PO_4)_2$-added samples than for the filler-free sample at 60°C. Thermal analysis showed that PEO/$Ca_3(PO_4)_2$/$LiClO_4$ electrolytes were thermally stable up to 180°C. The values of both $\tau_3$ and $V_f$ increased with an increase in the salt concentration in the low-concentration region; this was attributed to filler/salt interaction. The correlation between the critical $V_f$ and ionic conductivity as a function of the temperature and cycling behavior of the $LiFePO_4$/NCPE/Li cells will be published in a future communication.

## References


1. Tarascon, J. M.; Armand, M. Nature 2001, 414, 359.
2. Meyer, W. H. Adv Mater 1998, 10, 339.
3. Wright, P. V. Electrochim Acta 1998, 43, 1137.
4. Song, J. Y.; Wang, Y. Y.; Wan, C. C. J Power Sources 1999, 77, 183.
5. Manuel Stephan, A. Eur Polym J 2006, 41, 21.
6. Manuel Stephan, A.; Muniyandi, N.; Renganathan, N. G.; Karan, R. T. Solid State Ionics 2001, 130, 123.
7. Mancini, M. L. G.; Hanrath, T.; Teeters, D. Solid State Ionics 2000, 135, 283.
8. Manuel Stephan, A.; Nahm, K. S. Polymer 2006, 47, 5952.
9. Appetecchi, G. B.; Croce, F.; Persi, L.; Ronci, F.; Scrosati, B. J Electrochem Soc 2000, 147, 4448.
10. Croce, F.; Appetecchi, G. B.; Perci, L.; Scrosati, B. Nature 1998, 394, 456.
11. Andrew, Y. G.; Bruce, P. G. Electrochim Acta 2000, 45, 1413.
12. Shin, J. H.; Alessandrini, F.; Passerini, P. J Electrochem Soc 2005, 152, A283.
13. Manuel Stephan, A.; Prem Kumar, T.; Nathan, M. A. K.; Angulakshmi, N. J Phys Chem B 2009, 113, 1963.
14. Thomas, S.; Thomas, S. J Phys Chem C 2009, 113, 97.
15. Evans, J.; Vincent, C. A.; Bruce, P. G. Polymer 1987, 28, 2324.
16. Appetecchi, G. B.; Croce, F.; Scrosati, B. Electrochim Acta 1995, 40, 991.
17. Chusid, O; Gofer, Y.; Aurbach, D.; Watanabe, M.; Momma, T.; Osaka, T. J Power Sources 2001, 97–98, 632.
18. Ribeiro, R.; Silva, G. G.; Mohallen, N. D. S. Electrochim Acta 2001, 46, 1679.
19. Shodai, T.; Owens, B. B.; Ostsuka, M.; Yamaki, J. J Electrochem Soc 1994, 141, 2978.
20. Thomas, S. P.; Thomas, S.; Bandyopadhyay, S. J Phys Chem C 2009, 113, 97.
21. Xu, K. Chem Rev 2004, 104, 4303.
22. Chu, P. P.; Reddy, M. J.; Kao, H. M. Solid State Ionics 2003, 156, 141.
23. Chiang, C. Y.; Reddy, M. J.; Chu, P. P. Solid State Ionics 2004, 175, 631.
24. Appetecchi, G. B.; Hassoun, J.; Scrosati, B.; Croce, F.; Cassel, F.; Salomon, M. J Power Sources 2003, 124, 246.
25. Croce, F.; Curini, R.; Marginally, A.; Persi, L.; Ronci, F.; Scrosati, B.; Caminiti, R. J Phys Chem B 1999, 103, 10632.
26. Croce, F.; Persi, L.; Scrosati, B.; Flory, F. S.; Plichta, E.; Hendrikson, M. A. Electrochim Acta 2001, 46, 2457.
27. Wieczorek, W.; Such, K.; Wycislik, H.; Plocharski, J. Solid State Ionics 1989, 36, 255.
28. Capiglia, C.; Mustarelli, P.; Quatarone, E.; Tomasi, C.; Magistris, A. Solid State Ionics 1999, 118, 73.
29. Wieczorek, W.; Florjancyk, Z.; Stevens, J. R. Electrochim Acta 1995, 40, 2251.
30. Przluski, J.; Siekierski, M.; Wieczorek, W. Electrochim Acta 1995, 40, 2101.
31. Immanuel Selvaraj, I.; Chklanobis, S.; Chandrasekhar, V. J Electrochem Soc 1995, 142, 366.
32. Manuel Stephan, A.; Anbu Kulandainathan, M.; Renganathan, N. G. Eur Polym J 2005, 41, 21.
33. Bruce, P. G.; Hardgrave, M. T.; Vincent, C. A. Solid State Ionics 1992, 53–56, 1087.
34. Cameron, G. G.; Ingram, M. D.; Harvie, J. L. Faraday Discuss Chem Soc 1989, 88, 55.
35. Pearson, F. G.; Marchessault, R. H.; Liang, C. Y. J Polym Sci 1960, 43, 101.
36. Ramesh, S.; Yuen, T. H.; Shen, C. J. Spectrochim Acta A 2008, 69, 670.
37. Hodge, R. H.; Bastow, T. J.; Edward, G. H.; Simon, G. P.; Hills, A. J. Macromolecules 1996, 29, 8137.
38. Wang, C. L.; Maurer, F. H. Macromolecules 1996, 29, 8249.
39. Wen, S. J.; Richardson, T. J.; Ghantous, D. I.; Striebel, K. A.; Ross, P. N.; Cairns, E. J. J Electroanal Chem 1996, 408, 113.
40. Frost, R. L.; James, D. W.; Apple, R.; Meyer, M. J Phys Chem B 1982, 86, 3840.
41. Furtado, C. A.; Silva, G. G.; Machado, J. C.; Pimenta, M. A.; Silva, R. A. J Phys Chem B 1999, 103, 7102.
42. Elwell, R. J.; Pethrick, R. A. Eur Polym J 1990, 26, 853.
43. Forsyth, M.; Meakin, P.; MacFarlane, D. R.; Hill, A. J. J Phys Condens Matter 1965, 77, 601.
44. Hill, A. J.; Zipper, M. D.; Tant, M. R.; Stack, G. M.; Jordan, T. C.; Shultz, A. C. J Phys Condens Matter 1996, 8, 3811.
45. Peng, Z. L.; Bowing, S.; Li, S. Q.; Wang, S. J. J Appl Phys 1995, 334, 7711.